Journal of Alloys and Compounds 619 (2015) 676–680

Contents lists available at ScienceDirect

Journal of Alloys and Compounds

journal homepage: www.elsevier.com/locate/jalcom

Influence of deposition temperature on the microstructure and thermoelectric properties of antimonide cobalt thin films prepared by ion beam sputtering deposition

Zhuang-hao Zheng [a,b], Ping Fan [a,b,*], Guang-xing Liang [a], Dong-ping Zhang [b]

[a] College of Physics Science and Technology, Institute of Thin Film Physics and Applications, Shenzhen University, 518060, China
[b] Shenzhen Key Laboratory of Sensor Technology, Shenzhen 518060, China

ARTICLE INFO

Article history:
Received 21 August 2014
Received in revised form 10 September 2014
Accepted 10 September 2014
Available online 18 September 2014

Keywords:
Thermoelectric properties
Thermoelectric thin film
Antimonide cobalt

ABSTRACT

Antimonide cobalt thin films were deposited on BK7 glass substrates at various substrate temperatures by ion beam sputtering deposition with a fan-shape target. The influence of deposition temperature on the microstructure and thermoelectric properties of antimonide cobalt thin films were systematically investigated. It is found that the Seebeck coefficient of the thin film increases at first and then decreases with the increasing deposition temperature. The Seebeck coefficient of the sample deposited at 250 °C has maximum value and increases stably when the measuring temperature increased from room-temperature to 600 K. The electrical conductivity of the thin film increases significantly to 5.6×10^4 S cm^{-1} when the deposition temperature was 450 °C and then decreases greatly when the temperature increased to 500 °C and 550 °C. The behavior of electrical conductivity of the sample deposited at 250 °C changes from metallic to semiconducting after the measuring temperature exceeded 540 K. The power factor of antimonide cobalt thin film deposited at 250 °C has a maximum value of 0.93×10^{-4} W m^{-1} K^{-2} at room-temperature and then increases to 3.5×10^{-4} W m^{-1} K^{-2} when the measuring temperature was 540 K.

1. Introduction

Thermoelectric generator are great interest because of their widely applications in energy resources, semiconductor cooling and temperature sensors [1,2]. But they are relegated to niche applications due to the poor energy conversion efficiency of thermoelectric materials [3,4]. The energy conversion efficiency of thermoelectric material is determined by the dimensionless figure of merit (ZT) which is defined as $S^2T\sigma/\kappa$, where S is the Seebeck coefficient, T is the absolute temperature, σ is the electrical conductivity and κ is the thermal conductivity [5]. Researching new techniques for preparing high ZT value thermoelectric materials is extremely urgent. Antimonide cobalt based materials, such as $CoSb_3$ skutterudite, exhibit good value of Seebeck coefficient and electrical conductivity, hence are promising high ZT values [6,7]. For instance, Shi et al. [8] have report that the $CoSb_3$ filled $Ba_{0.08}La_{0.05}Yb_{0.04}$ has highest ZT of 1.7 at 850 K. However, its thermoelectric properties are still inadequate for practical use and further improvement in thermoelectric properties is vital for its large scale application. In particular, thin film technique is one of method to improve the thermoelectric properties of thermoelectric materials [9–11]. A high room-temperature figure of merit of $ZT = 2.4$ has been reported for P-type Bi_2Te_3/Sb_2Te_3 superlattices [12]. Recently, A few studies on the synthesis of antimonide cobalt based thin films have also been reported [13–16], such as Savchuk et al. [17] synthesized $CoSb_3$ thin films by magnetron DC-sputtering and investigated that the thin films have $ZT > 1$. However, it is still ignored comparing to the high thermoelectric properties bulk materials [18].

Ion beam sputtering deposition (IBSD) is a very attractive technique since it combines a high deposition rate with great versatility in depositing thin films [19]. In addition, preparing antimonide cobalt thin films by ion beam sputtering deposition is rarely reported. Therefore, in this work, antimonide cobalt thin films deposited by IBSD were studied. Instead of using alloy targets, a fan-shaped target was made of the Co target and Sb target combination. The influence of the deposition temperature on the microstructure, surface morphology and thermoelectric properties of the thin films were systematically investigated.

* Corresponding author at: College of Physics Science and Technology, Institute of Thin Film Physics and Applications, Shenzhen University, 518060, China. Tel.: +86 075 26536021.
E-mail address: fanping308@126.com (P. Fan).

http://dx.doi.org/10.1016/j.jallcom.2014.09.096
0925-8388/

2. Experimental

Ion beam sputtering deposition was used to deposit antimonide cobalt thermoelectric thin films on BK7 glass substrates. A fan-shaped target was made of high purity Sb (99.99%) and Co (99.99%) plates. The substrates were ultrasonically cleaned in acetone, alcohol and deionized water for 10 min, respectively. The chamber was pumped to a base pressure of 8.0×10^{-4} Pa and the working pressure was kept at 6.0×10^{-2} Pa with Ar of 9 sccm as the working gas. Prior to deposition, a 15 min pre-sputtering process was performed to remove native oxides and contaminants on the surfaces of the Sb/Co target. The sputtering energy was kept at 1.0 KeV with the beam current of 10 mA and the deposition time was fixed at 30 min. In order to obtain high quality thin films, the substrate temperature had been added to 200 °C, 250 °C, 300 °C, 350 °C, 400 °C, 450 °C and 500 °C. The samples were denoted as S1, S2, S3, S4, S5, S6 and S7, respectively.

The structure of the prepared antimonide cobalt thin films was studied by X-Ray diffraction (XRD) technique with the conventional θ–2θ mode (D/max2500 Rigaku Corporation). The surface morphology and composition ratio of the antimonide cobalt thin films was obtained by scanning electron microscopy (Hitachi Corporation) with an energy dispersive X-ray spectroscopy (EDS). The carrier concentration and mobility were measured by Van der Pauw Hall measurements at room-temperature (ET9000). The thermoelectric properties of the antimonide cobalt thin films were measured by the four-probe technique and Seebeck coefficient measurement system (SDFP-I) with the temperature gradient method (ΔK = 20 K). The thickness of the antimonide cobalt thin films was obtained by using a DEKTAK ST surface-profile measurement system.

3. Results and discussion

Table 1 shows the element content and the thickness as a function of deposition temperature. It can be seen that the thickness of the thin film decreases with the increasing deposition temperature. The composition of Co is less at low temperature and high temperature. But it closes in the middle temperature. XRD patterns of antimonide cobalt thin films are shown in Fig. 1. It is found that sample S1 and S2 mainly exhibit the Sb phase due to the highest dominated peak is from the diffraction of the Sb (0 1 2) plane. Some peaks locate at ~31°, ~42° and 52° is related to the $CoSb_3$ phase which indicates that the $CoSb_3$ is the secondary phase of the thin films. Besides this, few extra diffraction peaks are confirmed as $CoSb_2$ phase. But the intensity of those peaks is very weaker than others. When the substrate temperature increased to 300 °C, the peaks of S3–S6 relate to Sb (0 1 2) phase is disappeared and the intensity of the diffraction peaks locate at ~32° and ~34° rapidly increase. They are corresponding to the $CoSb_2$ phase and become to the mainly diffraction peaks of the thin films. Though some diffraction peaks relate to Sb and $CoSb_3$ phase are still observed, their intensity is much smaller than those peaks. This indicates that $CoSb_2$ is the dominant phase of the thin films deposited at 300–450 °C. However, the Sb phase appears to be the dominated phase and the $CoSb_3$ become the secondary phase again since the thin film was prepared at the substrate temperature of 500 °C. From the XRD results, it can be concluded that antimonide cobalt thin films with Sb and $CoSb_3$ mixed phase are obtained when the thin films deposited at low temperate. Then, they are translated to be $CoSb_2$ phase which can be consider as the single phase of the thin films when the temperature increased above 300 °C. Finally, the structure of the thin film resumes to Sb and $CoSb_3$ mixed phase at 500 °C which is similar to the thin films deposited at low temperature.

The effect of deposition temperature on the surface topography of the antimonide cobalt thin films was examined by the SEM plain-view and the corresponding photographs are shown in Fig. 2. The grains of S1 and S2 are irregular due to the contribution of $CoSb_3$ secondary phase. As the deposition temperature increased, the grains of S3 and S4 become uniform and the grains size decreases dramatically. Based on the XRD analysis, the grain size decrease can be speculated as the thin films gradually convert from mixed Sb and $CoSb_3$ phase to single $CoSb_2$ phases when the deposition temperature increased. Then, it can be seen that the grain size of S5, S6 and S7 tends to increase and transform to be mixed Sb and $CoSb_3$ phase again. The small size particle observed from S7 is suggested to be the separate of metallic Sb at much higher temperature.

Table 1
The composition and thin film thickness as a function of deposition temperature.

Deposition temperature (°C)	200	250	300	350	400	450	500
Co (%)	20.3	21.5	24.3	23.0	23.7	22.8	18.1
Sb (%)	79.7	78.5	75.7	77.0	76.3	77.2	81.9
Thickness (nm)	498	501	499	387	354	353	284

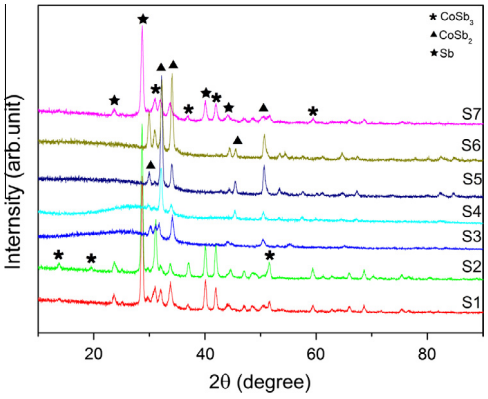

Fig. 1. XRD patterns of antimonide cobalt thin films.

Fig. 3 shows the carrier concentration and Hall mobility of the thin films as a function of substrate temperature. With the increased in deposition temperature, the carrier concentration increases and it has a highest value of 5.0×10^{19} cm^{-3} at the substrate temperature of 400 °C which will lead to higher electric conductivity. And then it decreases when the substrate temperature continued increasing to 400 °C. Though the carrier concentration of our thin films is less than that of the bulk [20], the carrier concentration of all the samples is in the range of 10^{18}–10^{19} cm^{-3}, this is the suitable carrier concentration range to achieve acceptable thermoelectric properties [21,22]. The Hall mobility of the sample deposited at 250 °C has the highest value and it is close to that of bulk. The Hall mobility of other samples is several times smaller than that of sample S2 (at 250 °C). Though sample S2 has a low carrier concentration, it has a large enough Hall mobility, which still results in acceptable electrical properties. In addition, higher mobility will always lead to a higher thermoelectric property [23]. Through XRD and surface topography analysis, it can be found that the sample has highest carrier concentration may due to the improvement of the crystal with a dominant phase of $CoSb_2$ phase and regular grain which will always with less defects. Sample S2 has higher Hall mobility and is evidently due to the decrease of gain boundaries with bigger grain size. In addition, $CoSb_3$ which has a special skutterudite structure is the secondary phase of the sample. The voids of $CoSb_3$ crystal can be filled with Sb ions that can decrease the carrier scattering and be effective to adjust higher mobility.

The Seebeck coefficient, electric conductivity and power factor ($PF = S^2\sigma$) of all the antimonide cobalt thin films measured at room-temperature are shown in Fig. 4. As can be seen from the figure, the positive S indicates that all the thin films are p-type semiconductor thermoelectric materials. The Seebeck coefficient of sample deposited at 250 °C has the highest value of 52 μV K^{-1} than that of others. It can be explained as that sample S2 with $CoSb_3$ crystal filling Sb ions has bigger effective carrier mass that can get bigger Seebeck coefficient. Then the Seebeck coefficient

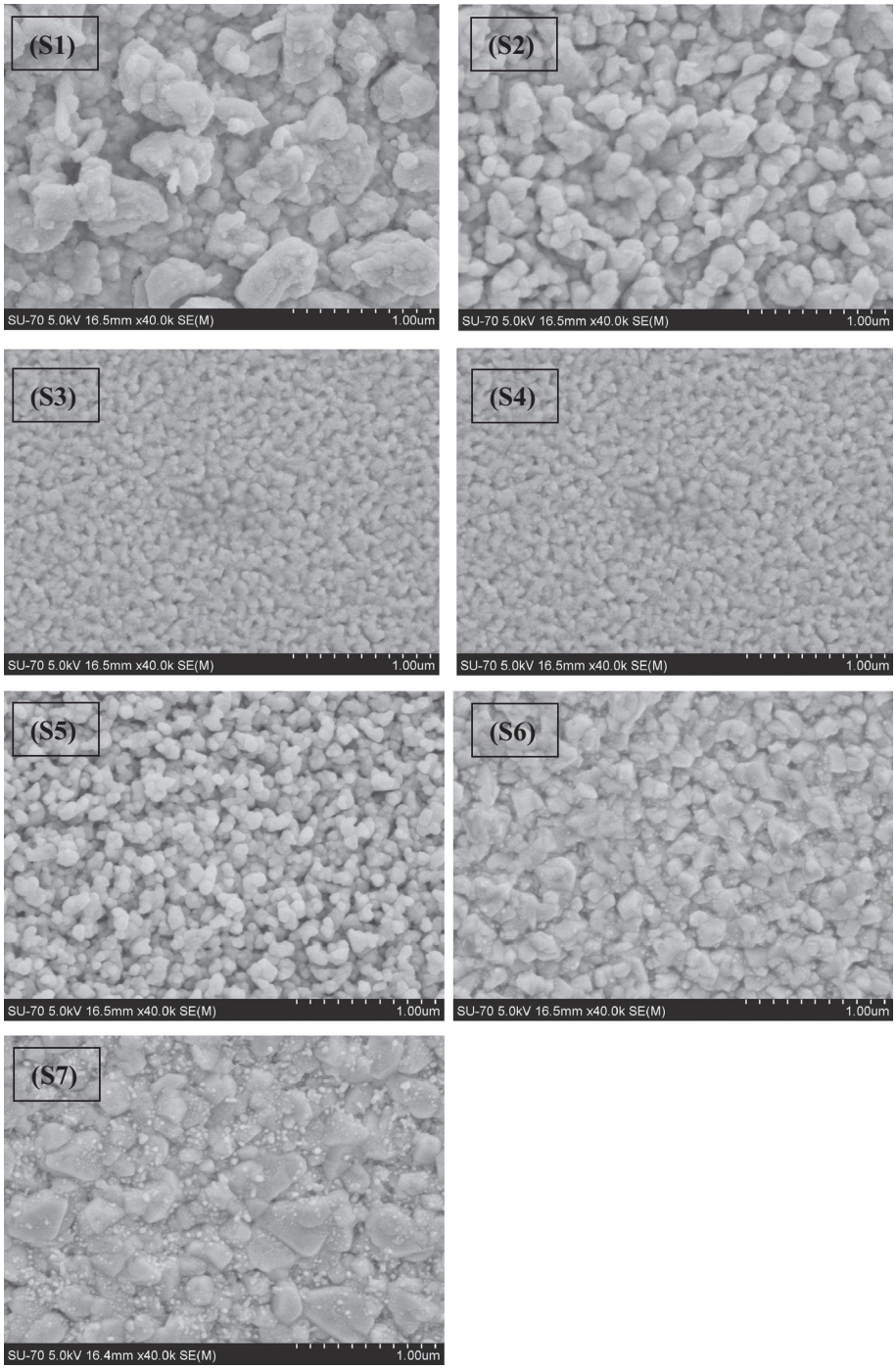

Fig. 2. The SEM plain-view of antimonide cobalt thin films. (S1) 200 °C, (S2) 250 °C, (S3) 300 °C, (S4) 350 °C, (S5) 400 °C, (S6) 450 °C and (S7) 500 °C.

decreases with the increased substrate temperature. It is due to the higher carrier density can cause a reduction in Seebeck coefficient [24]. With the increase of substrate temperature, the room-temperature electric conductivity of S1–S3 decreases when the phase transforms from mixed Sb and $CoSb_3$ phase to single $CoSb_2$ phase. When the substrate temperature was beyond a certain value, the electric conductivity enhanced. The electric conductivity of S5 (at 450 °C) has highest value of 5.6×10^4 S cm^{-1} due to its very high carrier concentration. The Power Factor which represents the electrical contribution to the overall thermoelectric performance is shown in Fig. 4. The room-temperature *PF* is at the range of 0.12×10^{-4}–0.93×10^{-4} W m^{-1} K^{-2} of our thin films. Sample S2 has the maximum *PF* with the highest Seebeck coefficient and a moderate electrical conductivity. It is several times than that of others, indicating that the thin film with mixed Sb and $CoSb_3$ phase has better thermoelectric properties than that of the thin films has single $CoSb_2$ phase.

It is reported that the antimonide cobalt material had better thermoelectric properties when the working temperature is above room-temperature [25]. So the temperature dependence on the Seebeck coefficient, electric conductivity and power factor of sample S2 is shown in Fig. 5. It can be observed that the electric conductivity of the thin film increases with the increased measuring temperature, indicating that the behavior of σ is basically

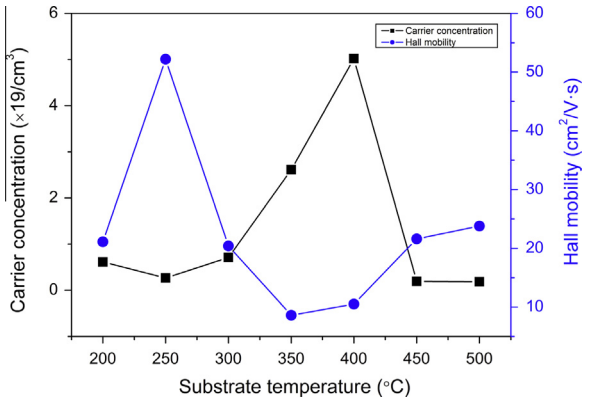

Fig. 3. Carrier concentration and Hall mobility of the antimonide cobalt thin films obtained as a function of substrate temperature.

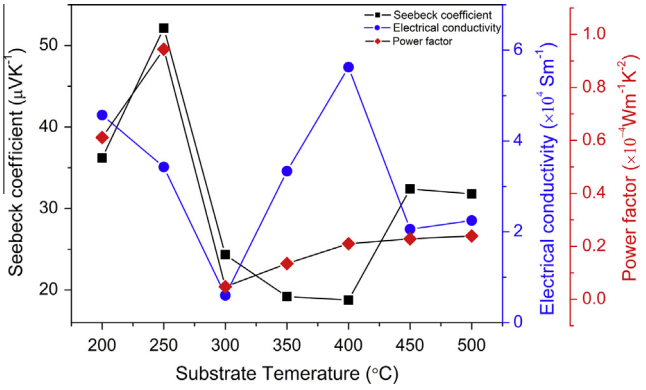

Fig. 4. Plot of Seebeck coefficient, electrical conductivity and power factors as a function of substrate temperature.

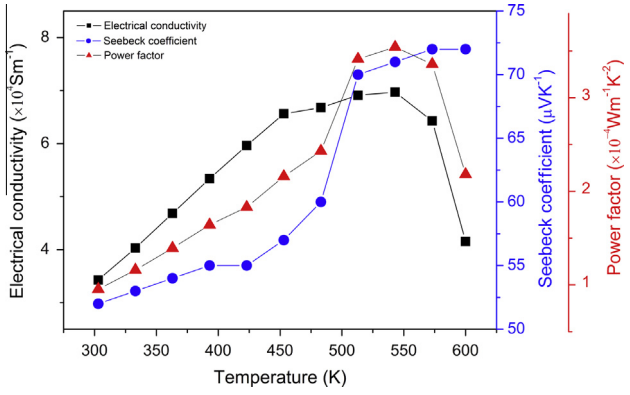

Fig. 5. The temperature dependence of Seebeck coefficient, electrical conductivity and power factors of sample S2.

metal-like due to the richness of Sb. However, when the measuring temperature is above 540 K, the σ decreases strongly and reaches to a small value, indicating that the behavior of σ changed from metallic to semiconducting. This effect might caused by the formation of $CoSb_2$ and the reduced of Sb after the temperature increased. In addition, the mobility will also reduce attribute to the depression in carrier transport due to the scattering by impurity surface oxidation and cause the reducing of electric conductivity. It is shown that the value of Seebeck coefficient enhances to 70 μV/K at the temperature of 500 K and then it slightly increases when the measuring temperature continued increasing. Generally, the Seebeck coefficient is inversely proportional to the carrier density. It can be consider as the reduction carrier density cause the enhancing Seebeck coefficient. The maximum *PF* of the thin film is 3.5×10^{-4} W m^{-1} K^{-2} at 540 K. Although this value is not as large as the reported value of antimonide cobalt bulk materials [14,17], the thermoelectric properties could increase because the thermal conductivity, κ, of antimonide cobalt thin films can be much lower than that of antimonide cobalt bulk materials [26,27].

4. Conclusions

Antimonide cobalt thin films were deposited by IBSD and the influence of deposition temperature on the properties is investigated. The prepared antimonide cobalt thin films show the mixed Sb and $CoSb_3$ phase at low deposited temperature and then transform to the dominant $CoSb_2$ phase when the deposition temperature were in the range from room-temperature to 500 °C. The grain sizes of antimonide cobalt thin films at first decrease and then increase with increasing deposition temperature. A highest electrical conductivity as large as 5.6×10^4 S cm^{-1} at room temperature is obtained when the thin film deposited at 450 °C, which has largest carrier concentration. But the Seebeck coefficient of this sample is very small. The *PF* of the thin film deposited at 250 °C has a highest value with a large Seebeck coefficient of 52 μV/K and a moderate value of electrical conductivity. It is several times than that of others, indicating that the thin film with mixed Sb and $CoSb_3$ phase has better thermoelectric properties than that of the thin films have $CoSb_2$ phase. Also, it increases when the measuring temperature increased and reaches to 3.5×10^{-4} W m^{-1} K^{-2} at 540 K.

Acknowledgements

Supported by Special Project on the Integration of Industry, Education and Research of Guangdong Province (2012B091000174) and Natural Science Foundation of SZU (Grant No. 201418).

References

[1] L.E. Bell, Science 321 (2008) 1457.
[2] P. Fan, Z.H. Zheng, Z.K. Cai, T.B. Chen, P.J. Liu, X.M. Cai, D.P. Zhang, G.X. Liang, J.T. Luo, Appl. Phys. Lett. 102 (2013) 033904.
[3] J.P. Heremans, V. Jovovic, E.S. Toberer, A. Saramat, K. Kurosaki, A. Charoenphakdee, S. Yamanaka, G.J. Snyder, Science 321 (2008) 554.
[4] D.M. Rowe, CRC Handbook of Thermoelectrics, CRC Press LLC, Boca Raton, London, New York, Washington, DC, 1995 (Chap. 3).
[5] D. Pinisetty, M. Gupta, A.B. Karki, D.P. Young, R.V. Devireddy, J. Mater. Chem. 21 (2011) 4098.
[6] B.C. Sales, D. Mandrus, R.K. Williams, Science 272 (1996) 1325.
[7] D.T. Morelli, G.P. Meisner, B. Chen, S. Hu, C. Uher, Phys. Rev. B 56 (1997) 7376.
[8] X. Shi, J. Yang, J.R. Salvador, M.F. Chi, J.Y. Cho, H. Wang, S.Q. Bai, J.H. Yang, W.Q. Zhang, L.D. Chen, J. Am. Chem. Soc. 133 (2011) 7837.
[9] L.D. Hicks, M.S. Dresslhaus, Phys. Rev. B 47 (1993) 16631.
[10] L.D. Hicks, M.S. Dresslhaus, Phys. Rev. B 47 (1993) 12727.
[11] M. Takashiri, K. Miyazaki, H. Tsukamoto, Thin Solid Films 516 (2008) 6336.
[12] R. Venkatasubramanian, E. Siivola, T. Colpitts, B. O'Quinn, Nature 413 (2001) 597.
[13] J.C. Caylor, A.M. Stacy, R. Gronsky, T. Sands, J. Appl. Phys. 89 (2001) 3508.
[14] J.C. Caylor, M.S. Sander, A.M. Stacy, J.S. Harper, R. Gronsky, T. Sands, J. Mater. Res. 16 (2001) 2467.
[15] D.V. Quach, R. Vidu, J.R. Groza, P. Stroeve, Ind. Eng. Chem. Res. 49 (2010) 11385.
[16] M. Daniel, M. Friedemann, N.J. hrmann, A. Liebig, J. Donges, M. Hietschold, G. Beddies, M. Albrecht, Phys. Status Solidi A 210 (2013) 140.
[17] V. Savchuk, A. Boulouz, S. Chakraborty, J. Schumann, H. Vinzelberg, J. Appl. Phys. 92 (2002) 5319.
[18] S.R. Sarath Kumar, Dongkyu Cha, H.N. Alshareef, J. Appl. Phys. 110 (2011) 083710.
[19] P. Fan, Z.H. Zheng, G.X. Liang, D.P. Zhang, X.M. Cai, J. Alloys Comp. 505 (2010) 278.
[20] T.M. Tritt, H. Bottner, L. Chen, MRS Bull. 33 (2008) 366.
[21] X. Chen, D. Parker, M.H. Du, D.J. Singh, New J. Phys. 15 (2013) 043029.

[22] W. Schweika, R.P. Hermann, M. Prager, J. Perßon, V. Keppens, Phys. Rev. B 99 (2007) 125501.
[23] Y. Kawaharada, K. Kurosaki, M. Uno, S. Yamanaka, J. Alloys Comp. 375 (2001) 193.
[24] R.C. Mallik, R. Anbalagan, K.K. Raut1, A. Bali, E. Royanian, E. Bauer, G. Rogl, P. Rogl, J. Phys.: Condens. Matter 25 (2013) 105701.
[25] C. Chubilleau, B. Lenoir, P. Masschelein, A. Dauscher, C. Candolfi, E. Guilmeau, C. Godart, J. Mater. Sci. 48 (2013) 2761.
[26] M.S. Dresselhaus, G. Chen, M.Y. Tang, R.G. Yang, H. Lee, D.Z. Wang, Z.F. Ren, J.P. Fleurial, P. Gogna, Adv. Mater. 19 (2007) 1043.
[27] N. V.-Schäuble1, T. Jaeger, Y.E. Romanyuk, S. Populoh, C. Mix, G. Jakob, A. Weidenkaff, Phys. Status Solidi RRL 7 (2013) 364.